

1N-46-CR
141367
p, 14

Semi-annual Progress Report for NASA grant NAG-1-1057

In situ detection of tropospheric OH, HO₂, NO₂, and NO
by laser-induced fluorescence in detection chambers at reduced pressures

For the period: 1 October, 1991 to 30 April, 1992

Principal Investigator: William H. Brune

Department of Meteorology
Pennsylvania State University
University Park, PA 16802

6 July, 1992

(NASA-CR-191916) IN SITU DETECTION
OF TROPOSPHERIC OH, HO₂, NO₂, AND
NO BY LASER-INDUCED FLUORESCENCE IN
DETECTION CHAMBERS AT REDUCED
PRESSURES Semiannual Progress
Report, 1 Oct. 1991 - 30 Apr. 1992
(Pennsylvania State Univ.) 14 p

N93-18599

Unclass

G3/46 0141367

This report is a brief summary of the status of work on the grant entitled "In situ detection of tropospheric OH, HO₂, NO₂, and NO by laser induced fluorescence in detection chambers at low pressures." The first version of the instrument has been essentially complete and operational for about six months, and we continue to make improvements on the instrument sensitivity and reliability. We are focusing our efforts on improving our understanding of the operating characteristics of the instrument – particularly the inlet transmission for OH and HO₂, the exact character of the air flow around and within the instrument, and the efficiency of the chemical conversion of HO₂ to OH. We are also in the process of converting this laboratory instrument into a field worthy instrument that we can take to remote sites for measurements.

Activities of the last six months

Instrument design and operation

The OH molecule is both excited and detected in the $A^2\Sigma(v'=0) \rightarrow X^2\Pi(v''=0)$ transitions near 308 nm, as opposed to exciting to the $A^2\Sigma(v'=1)$ state at 282 nm. Excitation at 308 nm produces substantially less laser-generated OH and organic molecule background fluorescence than excitation at 282 nm. At present, we tune the laser into resonance with the Q₁(3) transition at 308.24 nm, but we can use other transitions as well.

To separate the prompt scattering (Rayleigh and chamber scattering) from the OH fluorescence, we pull the ambient air into a detection chamber through an inlet, and maintaining the pressure of the cell at ~0.003 atm. With the quenching of the OH excited state reduced, the lifetime of the fluorescence extends beyond the laser pulse duration, and OH fluorescence can be detected after prompt scattering has ceased (called temporal filtering).

The instrument, shown schematically in Figure 1a, consists of a copper vapor laser-pumped dye laser that is frequency doubled into the ultraviolet and is multipassed through an evacuated detection chamber; a fast, gated detector with fast collection optics; a vacuum pump; and data collection electronics. The beam of ultraviolet laser light is focused into a White cell that has 24 passes (Figure 1b). The ultraviolet laser power is monitored at the exit of the White cell. This laser beam, with a repetition rate of 10 kHz, crosses the air stream in the center of the detection cell. At right angles to both the laser beam and the air flow is an optical train with fast, f#1 optics that focus the fluorescence onto a Hamamatsu microchannel plate detector, which has an 18 mm photocathode. The gain of the detector is normally reduced a factor of several thousand by a potential on a grid between the photocathode and the microchannel plates, but is turned on for 300 nanoseconds approximately 30 nanoseconds after each laser pulse has cleared the White cell.

The ambient air is introduced into the detection cell through a ~1 mm diameter hole, and the cell pressure is maintained at 2.4 Torr – 2 Torr from the atmosphere through the inlet, and 0.4 Torr from dry nitrogen or argon gas that is added at the White cell mirrors. The volumetric flow through the detection cell is 26 liters sec⁻¹. Nitrogen or argon gas is added to protect the White cell mirrors and to fill the volume of the detection chamber,

thus confining the atmospheric air to a relatively narrow stream ($\sim 1.7 \pm .5$ cm dia.) in the middle of the detection chamber. A loop inside the detection chamber, located 7-20 cm upstream of the detection axis, is used to add either NO for conversion of HO₂ to OH or C₃F₆ for removal of OH as a test of the background signal.

For an instrument based on the design of Hard and O'Brien, seven concerns must be addressed: sensitivity, minimum detectable OH, specificity, freedom from interference, calibration, OH/HO₂ inlet transmission, and detection of other species. The current status of our instrument for each one of these concerns will be briefly discussed here.

The sensitivity of the detection axis was calibrated directly by attaching a low-pressure, discharge-flow tube directly to the detection cell. Excess H atoms, produced in a microwave discharge or on a hot filament, were reacted with a known quantity of NO₂ to produce a known amount of OH. In September, 1991, the detection sensitivity, C, (given by the expression: $signal = C \times [OH]$) was 4×10^{-6} (cts sec⁻¹)/(OH molecule cm⁻³), with the assumption that the inlet transmission of OH was 100%. For measurements in March, 1992, the detection sensitivity was 1.3×10^{-5} (cts sec⁻¹)/(OH molecule cm⁻³). These sensitivities are obtained with average laser powers of 15 mW and 7 mW respectively, for which saturation of the OH transition is minimal. We believe that we can get another factor of five increase in sensitivity with the replacement of an interference filter. Our current detection sensitivity is better than the projections in our original proposal.

The minimum detectable OH is dictated by the background signal. For our analysis thus far, the background signal is proportional to laser power, with the exception of ~ 1 ct sec⁻¹ that is due to detector noise and 1-3 cts sec⁻¹ that is due to solar scatter. We believe that this background is due to the "ringing" of the detection chamber with Rayleigh and chamber scattering. In September, 1991, this background signal was 10-15 cts sec⁻¹; in April, 1992, it is 20-40 cts sec⁻¹, depending on the exact alignment the input beam into the White cell on a given day.

As a result, the minimum detectable OH, given by

$$[OH]_{min} = \frac{S/N \cdot \sqrt{2 \cdot S_{bkgnd}}}{C \cdot \sqrt{time}}$$

for $S/N = 2$ and $time = 30$ sec, was 5×10^5 cm⁻³ in September, 1991, and is 1.0×10^5 cm⁻³ in April, 1992, with a laser power of 15 mW and a background scattering signal of 30 cts sec⁻¹. (In five minutes, OH_{min} is about 3 times lower.) We anticipate that we will be able to decrease the minimum detectable OH by another factor of 2 to 5. This minimum detectable OH is adequate for OH and HO₂ measurements throughout the troposphere in a wide variety of conditions.

One of the advantages of a spectroscopic technique is that the spectrum is a unique fingerprint of the molecule. Both the wavenumbers and the intensities of the observed fluorescence spectrum give us information. The spectrum of OH, shown in Figure 2, comes from measurements of ambient HO₂ taken in September, 1991. This HO₂ was converted to OH by reaction with reagent NO, and the conversion efficiency for this measurement was considerably less than 100%, perhaps as low as only 5%. The Q₁(3), Q₂₁(3), and P₁(1)

lines are all evident, although the ratios are not correct because the ambient HO_2 abundance changed during the 2 minute spectral scan. We anticipate that with the improved instrument sensitivity we will obtain similar spectra for ambient OH in the summertime.

One of the serious concerns with this technique has been the laser generation of OH within the detection cell itself. We have measured this laser-generated OH with our current detection system. We used rather extreme conditions to test for this interference signal: both 300 ppbv of ozone and 3% of water vapor were added to a flow of dry air in the laboratory. The resulting OH signal was 2 ± 2 cts sec^{-1} . The laser power for this experiment was 0.025 watts, which is about 1.5- 2.5 times larger than we will use during measurements. Thus, laser generated hydroxyl is not an issue with this instrument.

We are measuring the interference signal from other gases. Atmospheric abundances of hydrogen peroxide produce negligible signals. As discussed below, the background signal is the same for measurements in the atmosphere as it is in the laboratory. This constancy indicates that non-resonant fluorescence from organic molecules or aerosols does not contribute significantly to the background signal for the environments tested.

The calibration of an instrument for measuring tropospheric hydroxyl is one of the most difficult aspects, once the sensitivity and specificity have been established. Our calibration to date is based on our low pressure calibration of the detection axis, with the assumption that the inlet transmission of OH and HO_2 is 100%. At present, this internal, low pressure calibration has an uncertainty of $\pm 30\%$.

To determine the inlet transmission, we need an external source of a known abundance of OH, so that the known, external OH abundance can be compared to the measured OH abundance derived from the internal calibration. What we require are several good calibration techniques for the entire instrument, including the inlet. We are working on these techniques, and propose to continue this work over the next three years.

We have only begun to understand the inlet transmission of OH and HO_2 in our system. We can assume that any hydroxyl radical that hits a surface of our instrument is chemically destroyed. Thus, it is our goal to design and operate a "wall-less" detection system. We can have broken the problem of the inlet design into three areas: external surfaces, the throat, and internal surfaces. We have begun to use suction through holes in the outer surface of the inlet to control the boundary layer, as shown in Figure 3a.

Internally, the air flow is a jet expansion, and because we add a small flow of argon to the detection chamber, the air flow is kept contained and away from wall surfaces, as shown in Figure 3b. We are currently optimizing the instrument for inlet diameter and distance between the inlet and the detection axis. These changes greatly affect the numbers in the figure, but the basic concept does not change. Any small recirculation that is occurring just inside the inlet can be controlled by the proper addition of an inert gas.

We are left with the problem of the possible losses in the throat itself, which can be tested by the combination of internal and external calibrations. However, the velocity in the instrument throat is roughly 300 m s^{-1} , and the possible contact time is only $10 \mu\text{sec}$ with the 3 mm thick inlet. A substantial transverse velocity, presumably generated by turbulence, of $> 100 \text{ m sec}^{-1}$ is required to mix much of the air to the throat surface in

this period of time.

One concern about this jet expansion is that the air stream gets cold for a short period, as can be seen in Figure 3b. Adducts may form at such low temperatures, and these possibilities need to be understood. Particular attention must be paid to the $\text{HO}_2\cdot\text{H}_2\text{O}$ adduct, which is thought to affect the disproportionation reaction of HO_2 . We are testing this possibility as we examine the conversion efficiency for the HO_2 to OH conversion. We do this test by converting external OH to HO_2 with the external addition of CO, allowing it to flow through the inlet, and converting it back to OH with reagent NO.

The last concern is the detection of the hydroperoxyl radical, HO_2 , by chemical conversion to OH by reaction with reagent NO, followed by LIF detection of the resulting OH. One of the difficulties in our high velocity system is that the mixing of reagent into the air stream and the chemical conversion of HO_2 to OH must occur in the same few milliseconds. This process can be accomplished by careful design of the NO injection system. Our current tests of changing the reaction time and the NO injector geometry show that excellent conversion efficiency ($> 90\%$) is possible. We are now working to implement those changes. However, further work will need to be done over the next six months to complete this development.

The high velocity and low air density in our system heavily favor the detection of HO_2 , without the detection of RO_2 . Model simulations show that RO_2 is rapidly converted to RO by reagent NO, but that the reaction between RO and O_2 to produce HO_2 is much slower. As shown in Figure 4, the RO_2 interference is below 6% when $[\text{HO}_2] = 0.5 \times [\text{RO}_2]$ for a reaction time of 2 msec. We intend to devise tests for RO_2 sensitivity during the next three years.

Detection of tropospheric OH and HO_2

We detected ambient OH during March, 1992, from the roof of the Walker Building, which houses our laboratory here at Penn State. The proportionality constant for the sensitivity was $1.5 \times 10^{-5} \text{ (cts sec}^{-1}\text{)}/(\text{OH cm}^{-3})$. With this system, we observed the signals for OH and HO_2 that are shown in Figure 5. The solid line is the signal in counts per second from the detection of the ambient air; the dotted line is from the resonance OH cell. The large signals are due to the addition of NO, and thus represent the HO_2 abundances. The conditions of the day were overcast skies, temperatures of about 35°C , and ozone and water vapor as shown.

The addition of hexafluoropropylene, denoted as C_3F_6 , removes OH and produces a background signal that is essentially identical to the off-resonance background.

If we assume that the inlet transmission of OH is 100%, and we use the chemical calibration, the approximate [OH] scale can be added to Figure 6. Thus we believe that on 18 March, 1992, in relatively clean air, that the ambient levels of OH in mid-afternoon were roughly $1 - 2 \times 10^6 \text{ molecules cm}^{-3}$. The 1σ statistical uncertainty of each data point is $\pm 1 \times 10^5 \text{ OH molecules cm}^{-3}$, giving a signal-to-noise ratio of 12; however, the absolute calibration is uncertain to about a factor of 2.

The hydroperoxyl radical was also measured occasionally by the addition of reagent NO to the air stream inside the nozzle. The mixing of NO into the air stream for the instrument configuration at that time was not well known. However, if we assume a conversion efficiency of 100%, then the HO₂ abundances were approximately $1 - 2 \times 10^8 \text{ cm}^{-3}$, or 4 to 8 pptv. The absolute accuracy of these numbers is probably a factor of two to three. The signal-to-noise ratio for HO₂ was 36 for 1 second.

These data demonstrate that we now have an instrument that has good sensitivity and specificity for the hydroxyl radical.

Planned activities for the next six months

We now have to improve our rough calibration, understand the inlet transmission of OH and HO₂ and the chemical conversion efficiency of HO₂ to OH, and build a field-worthy instrument based on the breadboard concept. We also intend to participate in field studies, both here at Penn State and at remote locations. Such exercises will lead to a better understanding of the instrument characteristics and to improved and more reliable instrument design.

Development of calibration techniques.

We will begin to develop and use a number of calibration techniques, including those already in use by other scientists. We have now on several occasions successfully calibrated our detection axis by attaching a low pressure, discharge flow tube directly to the detection chamber and using the fast reaction $H + NO_2 \rightarrow OH + NO$ to determine the signal from a known amount of OH. We now wish to compare this calibration to ones in which the OH is made at atmospheric pressure outside the instrument inlet.

Our first technique will be the photolysis of a known amount of water vapor by a known amount of ultraviolet light (185 nm from an Hg lamp) in a known amount of time. A laminar airflow is contained in a short tube, from which part of the flow is vented and part is captured by the instrument inlet. Water vapor will be measured with a chilled mirror hygrometer, the ultraviolet flux with a photodiode that has been compared to an absolutely calibrated power meter, and the exposure time by the known velocity and velocity profile of the air entering the detector inlet.

Hydroxyl abundances of 5×10^5 to 5×10^8 molecules cm^{-3} can be produced, according to the equation:

$$[OH] = [H_2O] \cdot \sigma_{H_2O} \cdot F_{185} \cdot \Delta t$$

where

$[H_2O]$ is the water vapor concentration equal to volume mixing ratios of .01% to 1%;

$\sigma_{H_2O} = 5 \times 10^{-20} \text{ cm}^2$ is the water vapor cross section at 185 nm;

$F_{185} = 10^{10} - 10^{11} \text{ photons cm}^{-2} \text{ sec}^{-1}$ is the photon flux from a mercury per ray lamp with an 185 nm interference filter;

$\Delta t = 0.2$ seconds for a 7.5 cm diameter flow tube, a 1 cm diameter UV beam, and an air flow rate of 200 STD $\text{cm}^3 \text{sec}^{-1}$.

We are building a prototype of this calibration system for this summer. By the beginning of 1993, the uncertainty by this technique should be less than 50%, and the ultimate uncertainty may be as low as 20%.

A second technique requires that we make OH abundances that are 100 to 1000 times larger than ambient, or in the range of 2×10^8 to 2×10^9 OH molecules cm^{-3} . In this case, we will build a calibration cell that has an OH absorption axis just above the instrument inlet. The OH source will be either photolysis of water vapor or of ozone in the presence of water vapor, using distributed light sources with light flux monitors. Air, exposed to the ultraviolet light, will flow in a laminar stream toward the exhaust manifold. The instrument inlet will sample a small fraction of the air from this chamber. A laser beam will be focused into a White cell and passed 40 times over a 25 cm long path. The laser linewidth will be narrowed to 0.04 cm^{-1} , so that the OH absorption coefficient is $\sim 4 \times 10^{-15} \text{ cm}^2$. By Beer's Law, the absorption signal for 1×10^9 OH molecules cm^{-3} is 0.004 of the initial intensity. This absorption can be measured with standard absorption techniques. Absolute uncertainties of less than $\pm 20\%$ are possible with this technique, but at an OH concentration that is higher than ambient.

Once these external and internal calibration techniques are both available, the inlet transmission for OH can be readily established. For a known external source, we simply compare the observed signal to that expected from the internal calibration. The ratio of external signal to expected signal from the internal calibration will give us the inlet transmission. We can always track this inlet transmission by measuring the relative OH signals from a point source of OH that can be placed both inside and outside the detection chamber during the absolute calibrations, and then later during actual measurements. We will also measure Rayleigh scattering, along with the measured laser power, to maintain the instrument calibration during field operation.

Air flow and chemical conversion of OH to HO₂

We have begun studies of the external air flow around the instrument inlet by the Schlieren technique. These studies produce qualitative pictures of the air flow, and indicate that suction through a number of holes on outer surface of the inlet may prevent air from contacting the outer surface and then entering the inlet. We are continuing to use the Schlieren technique for these studies of the outer surface of the inlet, and are planning to develop a system to study the internal flow as well, with an emphasis on finding possible recirculation of air inside the detection chamber.

We will also begin quantitative studies on the conversion efficiency of HO₂ to OH by reaction with reagent NO. In one method for determining the efficiency, we will make OH in the air stream entering the inlet. This OH will be converted to H and then HO₂ by the addition of CO to the flow. Once the air is inside the detection chamber, the HO₂ will be converted back to OH by reaction with reagent NO. The ratio of the converted OH signal

to the original OH signal is the conversion efficiency of the system times the ratio of the inlet loss of HO₂ to that of OH.

Field studies of OH and HO₂

We have been offered the opportunity to participate informally in the ROSE II (Rural Ozone of the Southern Environment). These measurements, which will be made in a rural pine forest in southwestern Alabama in June, 1992, should provide a severe test for this detection technique and for the equipment. We will learn, for instance, if the large hydrocarbon abundances add significantly to the background signal. We are going to attempt to make our measurements at a height of 6 meters. If we are successful, then we will be able to consider making measurements at even greater heights, perhaps even as high as 30 meters. In addition to this study, we also plan to make measurements with the same apparatus in agricultural land near State College some time in late September. We hope to correct any problems that may arise in Alabama and improve the detection sensitivity and instrument diagnostics.

These field measurements will speed the transition of this instrument from laboratory breadboard to reliable field instrument.

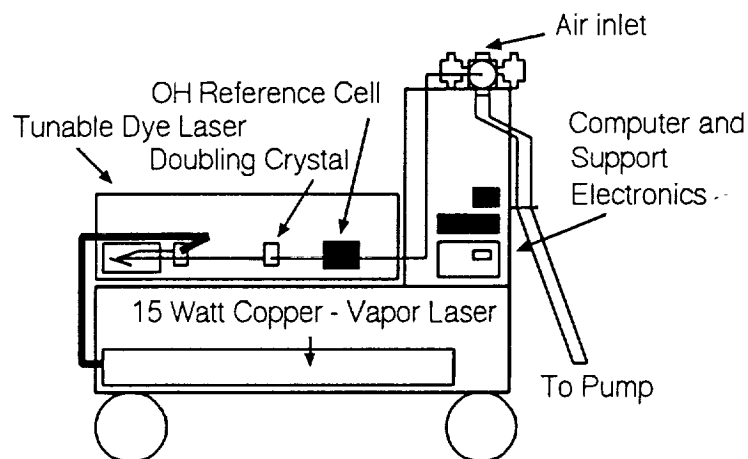
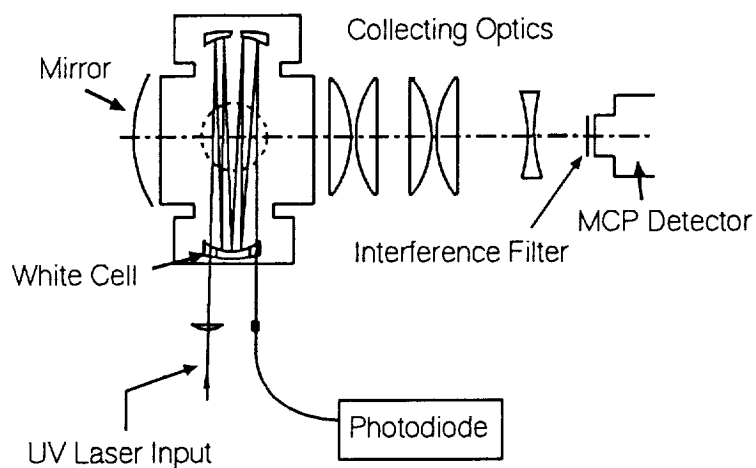


Figure 1. Schematic of the OH/HO₂ instrument. The general layout, shown in (a.), was used on the roof of the Walker building. The optical layout, which includes the White cell and the collecting optics leading to the microchannel plate detector (MCP PMT) are shown in (b.).

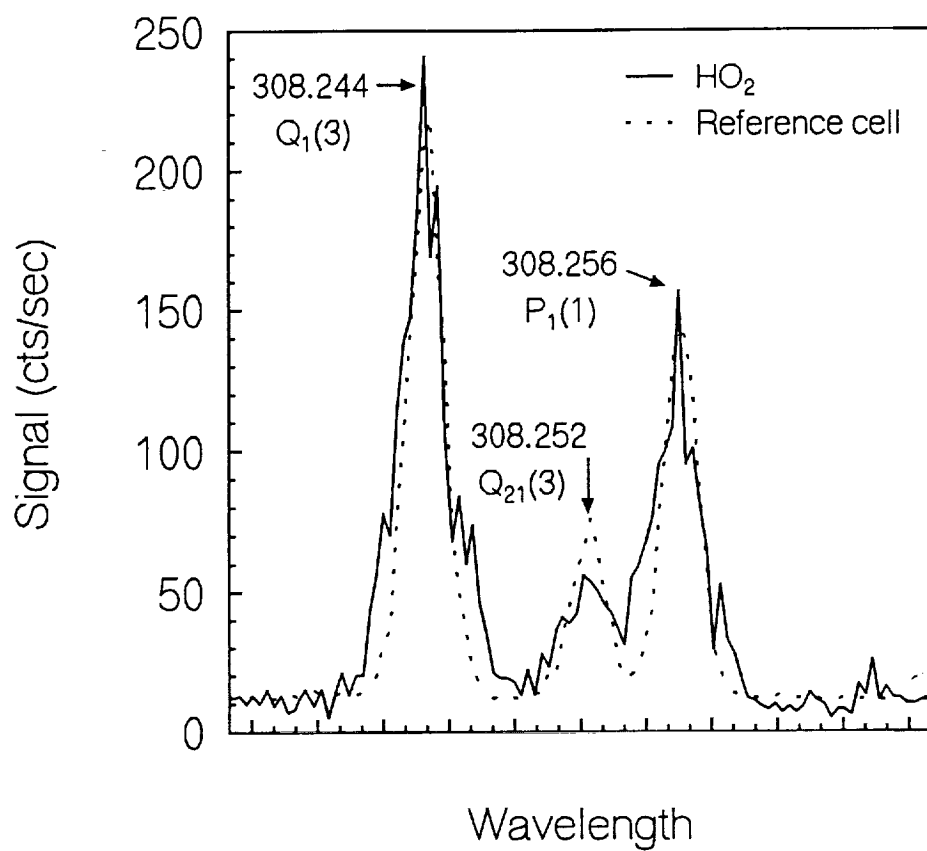


Figure 2. A partial OH spectrum of converted ambient HO₂, taken on 16 March, 1992. The reference cell signal is the dotted line. The ratio of the peaks is affected by the change in ambient HO₂, since the spectral scan took 2-3 minutes to complete.

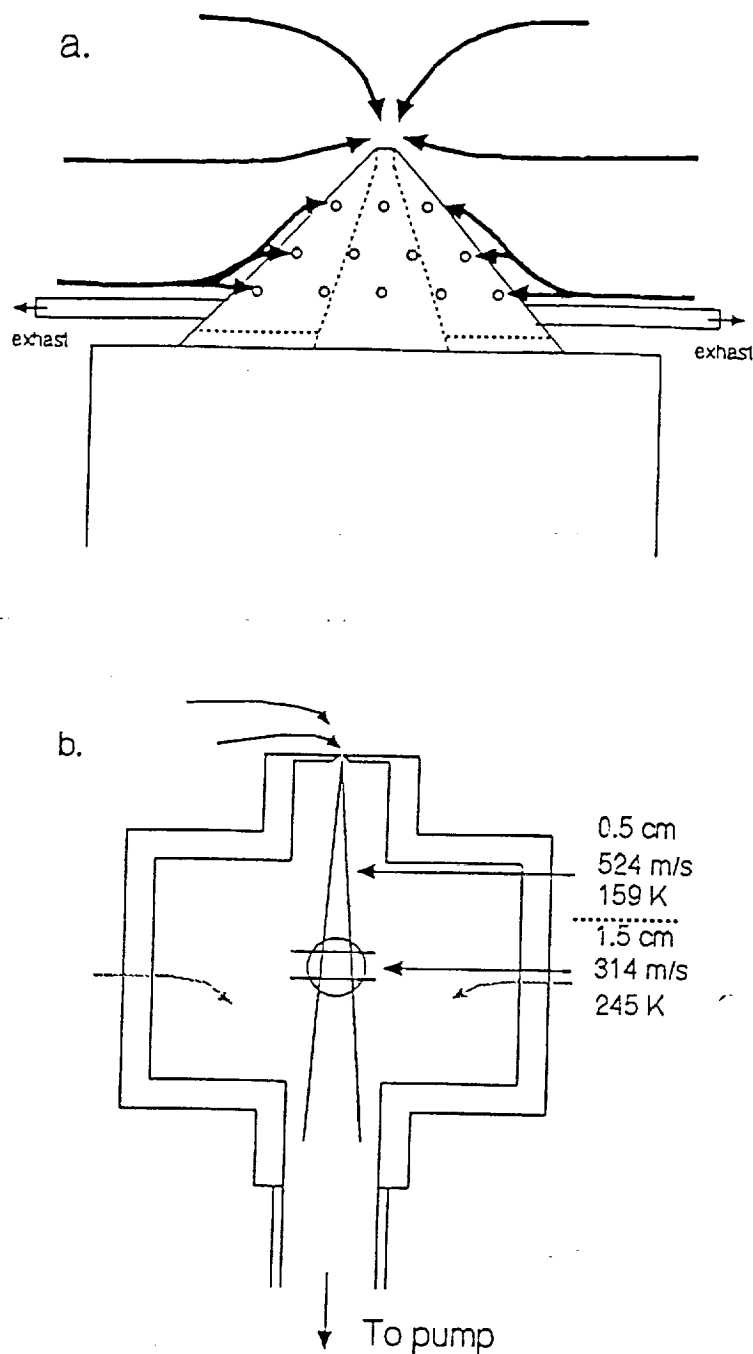


Figure 3. A schematic of an instrument inlet with suction (a.) produces the depicted air flow patterns. Measurements of the characteristics of the internal flow with a pitot tube and a fast thermistor are given for the inlet configuration shown in (b.). Notice the sharply defined air stream jet, the overlap with the laser beam (two horizontal lines) and the detector field-of-view (circle). Small flows of nitrogen are added near the White cell mirrors to keep them clean and to help confine the air stream.

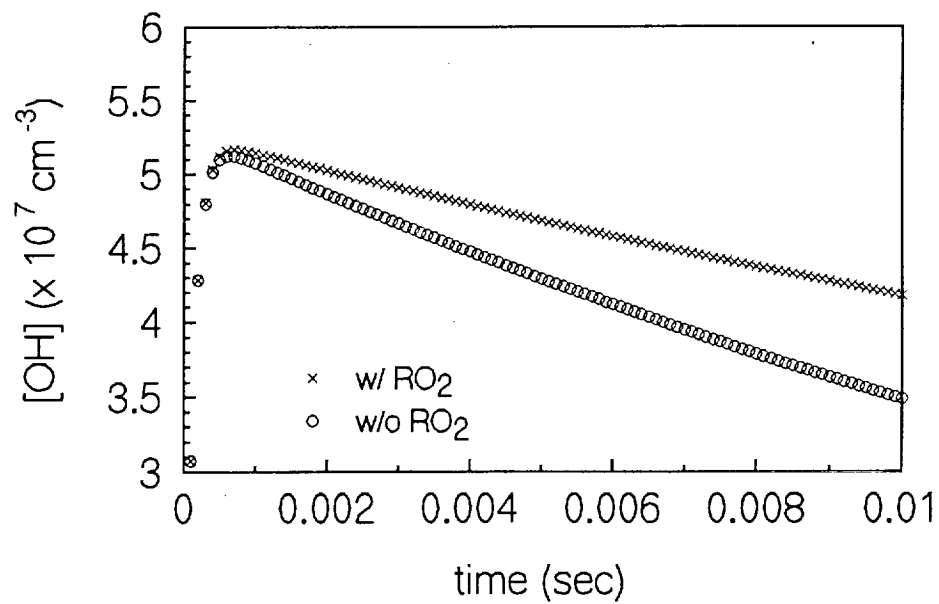


Figure 4. Calculation of the conversion of HO_2 and RO_2 to OH in our instrument. The RO_2 abundance is assumed to be twice the HO_2 abundance. The OH is detected $\sim 1 - 2$ msec after the addition point for NO . Only a few percent of the RO_2 is converted to OH .

OH/HO₂ measurement 3/18/92

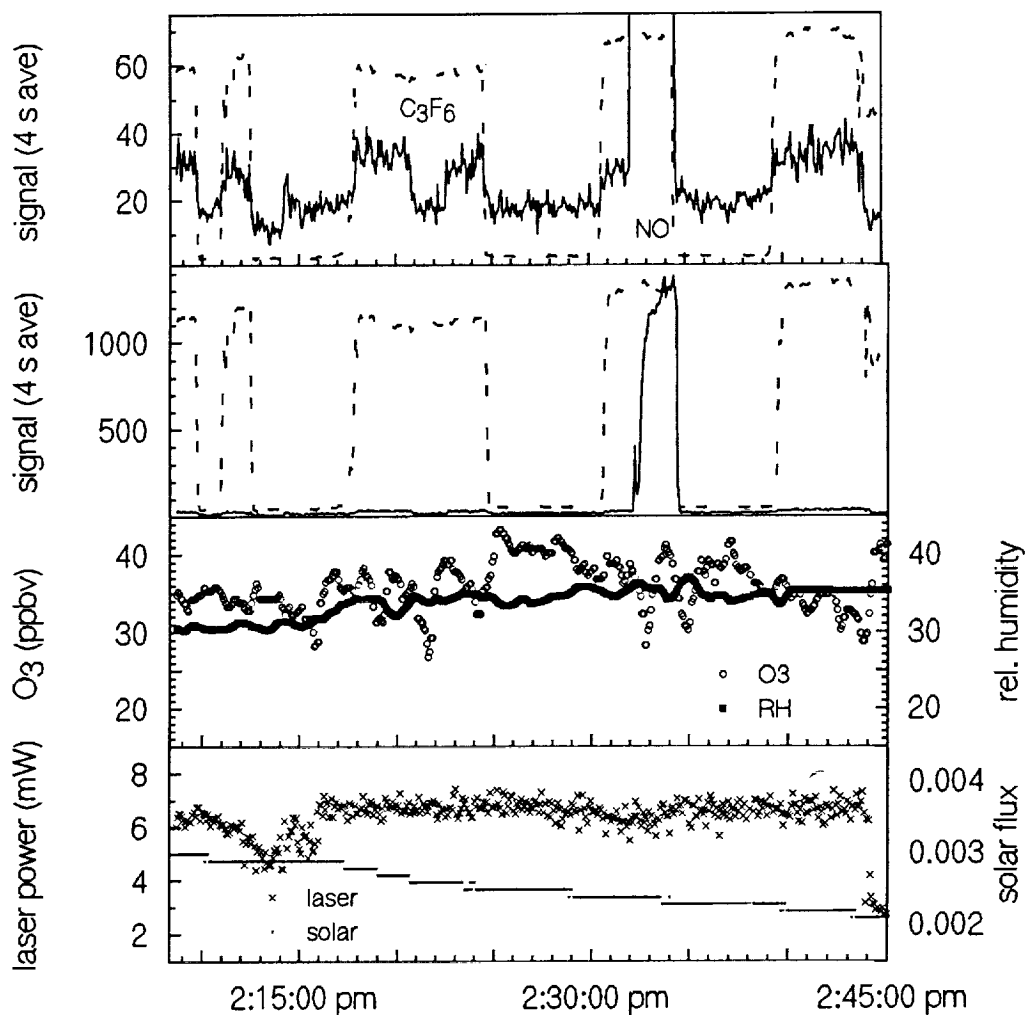


Figure 5. One segment of the OH/HO₂ abundance measurements from the roof of the Walker Building on 18 March, 1992. OH and HO₂ signals are shown for the instrument that now has better sensitivity and higher conversion efficiency of HO₂ to OH. The dashed line is the signal from the reference cell, indicating that the laser is on-line with the OH resonance when the signal is high.

OH/HO₂ measurement 3/18/92

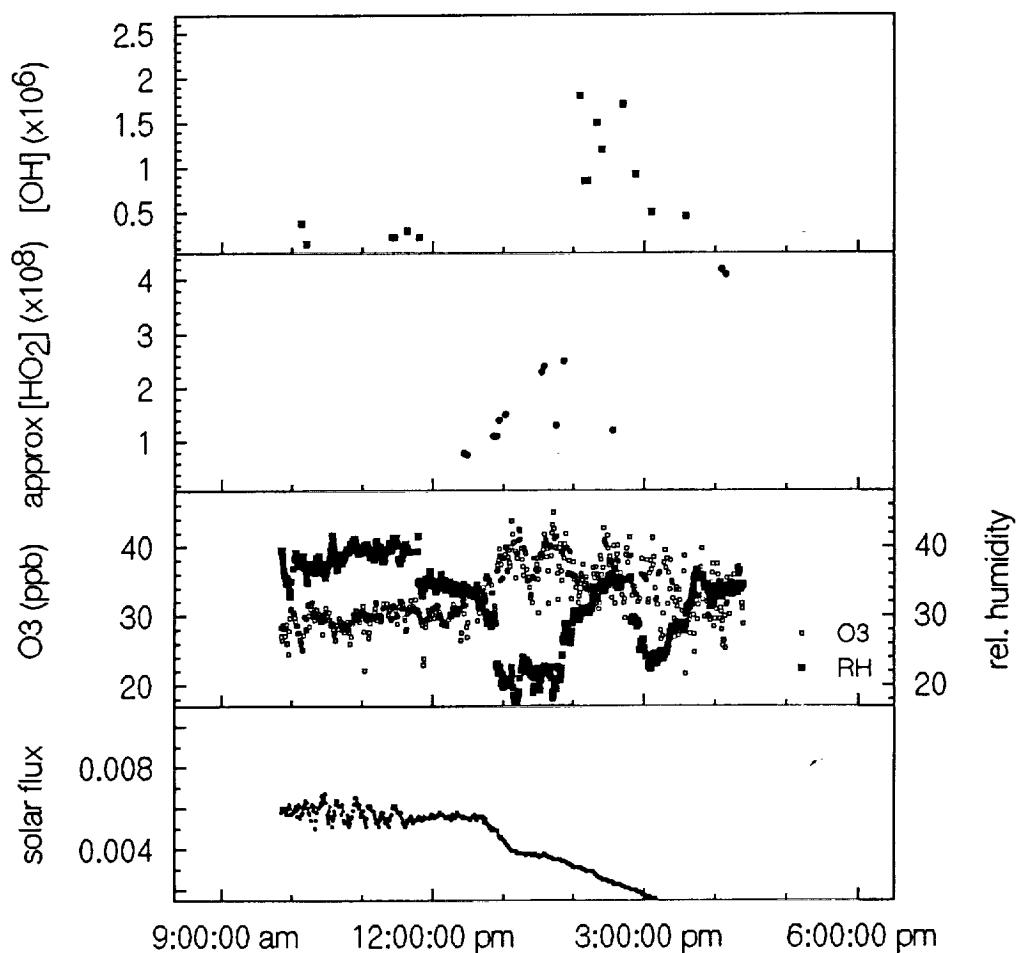


Figure 6. Measurements of OH and HO₂ for 18 March, 1992 from the roof of the Walker Building. Statistical uncertainties are less than one percent. Absolute uncertainties are approximately a factor of two to three. Shown also are the ozone mixing ratio, the relative humidity, and the total solar flux (in arbitrary units). The sudden rise in OH coincides with a frontal passage.